A Quasi-Optical Method for Measuring the Complex Permittivity of Materials

FRED I. SHIMABUKURO, MEMBER, IEEE, STEVEN LAZAR, MEMBER, IEEE, MICHAEL R. CHERNICK, AND HOWELL B. DYSON

Abstract —**A quasi-optical method for measuring the complex permittivity of materials is described. The determination is derived from measurements of the transmission of a perpendicularly polarized wave through a dielectric slab at different angles of incidence. This relatively simple method is quite sensitive. Accurate estimates of the relative permittivity and the loss tangent can be obtained by accurately measuring the frequency of the signal and by the use of large, precisely machined Fabry–Perot plates. Estimates of the standard errors in the determinations are obtained by using a bootstrap resampling technique. The measurements here are made at a frequency of 93.788 GHz at ambient temperature.**

I. INTRODUCTION

AT THE MILLIMETER wavelengths, waveguide, cavity, and various forms of quasi-optical methods are utilized to measure the complex permittivity of materials. Descriptions of the standard methods are given in [1], and descriptions of the modern methods, applicable in the millimeter and submillimeter wavelength ranges, are found in [2]–[5]. Bridges *et al.* [6] used two different waveguide measurement techniques to determine the permittivity and loss tangents of materials at 95 GHz: 1) by measuring the transmission through, and reflection from, a dielectric slab in waveguide, taking into account the multiple reflections between surfaces, and 2) by measuring the voltage standing wave ratio (VSWR) of a slab backed by a short, a technique described by Roberts and von Hippel [7]. Open resonators were first used to measure the dielectric properties of materials by Culshaw and Anderson [8], and subsequently by Degenford and Coleman [9]. Balanis [10] determined the permittivity and loss tangent at 60 and 90 GHz by placing a slab in a Fabry–Perot resonator and measuring the resonant spacing and the transmission of the dielectric loaded cavity, and reported errors of less than 1 percent for ϵ_r, and ± 15 percent for $\tan\delta$. Cullen and Yu [11] developed a theory for measuring permittivity using an open confocal resonator and this formed the basis for more accurate determinations of permittivity. Cook, Jones, and Rosenberg [12] compared cavity and open-resonator measurements of permittivity and loss angle (tangent) at 35 GHz. The agreement between the two methods was well within experimental error. Standard deviations obtained for ϵ_r and δ were 0.0021 and 2.1 μrad, respectively. Jones [13] further investigated the open resonator method for measuring dielectrics at 35 GHz and showed that, for materials with loss angles in the range of 50–500 μrad, the loss could be measured with a standard deviation of ± 2 percent+1 μrad, and the standard deviation in the determination of relative permittivity was ± 0.1 percent. In a straightforward quasi-optical method, Talpey [14] determined the complex permittivity of materials with unity permeability at 35.9 GHz by measuring the transmission of a parallel polarized wave through the sample dielectric slab at the Brewster angle. With a coherent source, a Michelson ([15]) or a Mach–Zehnder ([4], [16]) interferometer can be used to measure the relative permittivity, and for low-loss materials, this quantity can be measured to a few parts in 10^4 [2]. Using a broad-band source in conjunction with an interferometer, Fourier transform spectrometry can be utilized to derive the permittivity of materials [17]. Breeden and Shepherd [18] have used this technique in the range of 10–450 GHz to measure the relative permittivity of various materials. They report maximum errors of less than one percent in the determination of the relative permittivity. For broad-band applications, the most important method for the determination of the dielectric properties of materials has been dispersive Fourier-transform spectrometry (DFTS). This method was first described by Chamberlain *et al.* [19] and by Bell [20]. DFTS differs from conventional Fourier-transform spectrometry in the positioning of the dielectric sample. In the latter method, the sample is placed between the interferometer and the detector. In DFTS, the sample is placed in one arm of the interferometer and the ratio of the complex spectra obtained from the transformations of interferograms recorded with and without the sample gives both the attenuation and phase shift caused by the sample. It is seen that a single measurement determines the relative permittivity and loss tangent. Using this method, precise determinations of the complex permittivity of low-loss polymers have been made by Birch *et al.* [21] and by Afsar *et al.* [4]. Errors in the range 0.1 percent for ϵ_r, and 2 percent for $\tan\delta$ are quoted for the DFTS method.

Manuscript received November 3, 1983; revised February 27, 1984. This work was supported by the U.S. Air Force under Contract FO4701-83-C-0084.

F. I. Shimabukuro, S. Lazar, and H. B. Dyson are with the Electronics Research Laboratory, Laboratory Operations, The Aerospace Corporation, El Segundo, CA 90245.

M. R. Chernick is with the Concept Engineering Office, Engineering group, The Aerospace Corporation, El Segundo, CA 90245.

Waveguide and closed-cavity methods use small samples, and the closed systems eliminate diffraction effects and undesirable reflections from extraneous sources. However, at the shorter millimeter wavelengths, precision machining of the slab is required for exact fitting into the waveguide and cavity, and measurement difficulties arise if the wall losses become comparable or exceed the dielectric losses. Quasi-optical methods require large dielectric samples, and care must be exercised to correct for diffraction effects and to eliminate extraneous reflections into the measurement path. However, the method can be extended through the submillimeter to optical wavelengths. In this paper, we describe a quasi-optical method in which the complex permittivity is determined at 93.788 GHz by measuring the transmission of a perpendicularly polarized wave through a dielectric slab acting as a solid etalon, at different angles of incidence.

II. Formulation

The reflection and transmission coefficient of a solid etalon can be calculated by solving a well-known boundary value problem. For example, taking into account the complex permittivity and the angular dependence, a derivation is found in [22]. The transmission coefficient of a plane electromagnetic wave through a lossy dielectric slab incident at an angle θ is given by

$$T = \frac{(1-r^2)e^{-j(\beta_1-\beta_0)d}}{1-r^2e^{-2j\beta_1 d}} \tag{1}$$

where

$$\beta_1 = \frac{2\pi}{\lambda_0}\sqrt{\epsilon_1/\epsilon_0 - \sin^2\theta}$$

$$\beta_0 = \frac{2\pi}{\lambda_0}\cos\theta$$

$$\epsilon_1 = \epsilon_r\epsilon_0\left(1 - j\frac{\sigma}{\omega\epsilon_r\epsilon_0}\right)$$

and

ϵ_0	permittivity of free space,
ϵ_r	relative permittivity,
σ	conductivity,
λ_0	free-space wavelength,
$\frac{\sigma}{\omega\epsilon_r\epsilon_0}$	$\tan\delta$ = loss tangent,
d	slab thickness,

and r is the reflection coefficient of a plane electromagnetic wave incident on a dielectric boundary. For parallel polarization:

$$r = r_{\parallel} = \frac{\beta_1 - (\epsilon_1/\epsilon_0)\beta_0}{\beta_1 + (\epsilon_1/\epsilon_0)\beta_0} \tag{2}$$

and for perpendicular polarization

$$r = r_{\perp} = \frac{\beta_0 - \beta_1}{\beta_0 + \beta_1}. \tag{3}$$

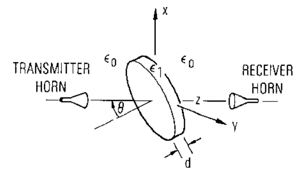

Fig. 1. In the measurement geometry shown, a perpendicularly polarized wave is incident on a dielectric slab at an angle θ.

For completeness, the slab reflection coefficient is given by

$$R = \frac{r(1-e^{-2j\beta_1 d})e^{2j\beta_0 d}}{1-r^2e^{-2j\beta_1 d}}. \tag{4}$$

The slab power transmission and reflection coefficients are given by $|T|^2$ and $|R|^2$, respectively. A schematic of the experiment is shown in Fig. 1. for the coordinate system shown, the slab is rotated about the y-axis.

III. Experimental Results

For the transmission experiments described here, a perpendicularly polarized incident wave was transmitted. Off normal incidence, $r_{\perp}$ increases with angle θ, whereas $r_{\parallel}$ decreases with θ until the Brewster angle, from where it increases to unity at grazing. It is seen that $r_{\perp} \geqslant r_{\parallel}$ for all angles of incidence. From (1) the contrast, the ratio of an adjacent transmission maximum and minimum, increases with reflectivity and so the use of a perpendicularly polarized wave gives a more accurate measure of the angular position of the transmission peaks and valleys, and thereby that of the real part of the permittivity. As an example, at a frequency of 93.8 GHz, $r_{\parallel}$ and $r_{\perp}$ are plotted for a TPX dielectric boundary in Fig. 2. Fig. 3 shows the power transmission coefficients through a 0.498-in-thick TPX sample for both polarizations. For low-loss dielectrics, the effects of the real part of the permittivity and the loss tangent are almost independent. The loss tangent primarily affects the amplitude level of the slab transmission curve, whereas the relative permittivity determines the angular location of the transmission maxima and minima. An indication of the sensitivity of the measurements is given by the quantities

$$\frac{\partial|T|^2}{\partial(\tan\delta)}$$

and

$$\frac{\partial\theta_{\max}}{\partial\epsilon_r}.$$

For the material TPX above

$$\frac{\partial|T|^2}{\partial(\tan\delta)}(\theta = \theta_{\max}) = 40.5 \tag{5}$$

and

$$\frac{\partial\theta_{\max}}{\partial\epsilon_r}(\theta = \theta_{\max}) = 70 \tag{6}$$

where $\theta_{\max}$ is a the angular position of the first transmission maximum. A change of 10^{-3} in the loss tangent

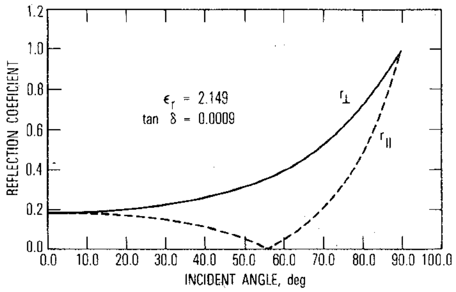

Fig. 2. The reflection coefficients for a perpendicularly ($r_\perp$) and parallel ($r_\parallel$) polarized waves at a TPX dielectric boundary are shown.

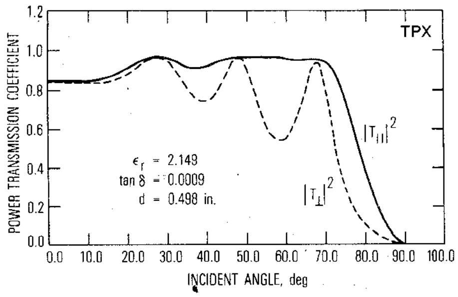

Fig. 3. The power transmission coefficients through a 0.498-in-thick TPX slab for perpendicularly and parallel polarized waves are shown.

changes the peak transmission by 4 percent, and a change of 10^{-2} in the relative permittivity shifts the position of the transmission maximum by 0.7°. It is seen that this method has good sensitivity for the measurement of the complex permittivity of materials. A photograph of the essential elements of the experiment is shown in Fig. 4. During the actual measurements, pieces of absorbing material were strategically placed around the experiment to eliminate extraneous reflections into the measurement path. The only significantly noticeable extraneous reflections occurred at incident angles near zero degrees and these were due to the multiple reflection interaction between the dielectric sample and the receiving horn. These extraneous reflections increase the standard error in the estimates of the complex permittivity.

The dielectric samples consisted of four-in-diam disks, machined to a flatness ±0.001 in on both sides, and ranged in thickness from 0.389 to 0.740 in. The thickness could be measured to within ±0.001 in. The holder for the dielectric samples was fabricated out of teflon and mounted on a precision rotary stage. The angles of incidence were set manually to an estimated error of less than 0.25°. Because of foreshortening effects, useful transmission data could be obtained only to incident angles of about 50°. At that point, deleterious reflection effects of the holder could be detected. In the experiment, the power transmission coefficients through the different dielectric slabs were measured at 1° increments of incident angles from 0° to 50° for each of the samples, except for herasil; for this case, the transmission measurements were made to a maximum incident angle of 40°. The signal source was a fixed tuned Gunn oscillator whose frequency was measured to less than one MHz by down converting into a frequency counter. The signal frequency drift during the measurements was less than 10 MHz, and so the operational wavelength was known to one part in 10^4.

The measured power transmissions of a 93.8-GHz perpendicularly polarized wave at different incident angles through various dielectrics are shown in Fig. 5(a)–(h). Besides those of the commonly used dielectric materials at the millimeter wavelengths, teflon, rexolite, and TPX, mea-

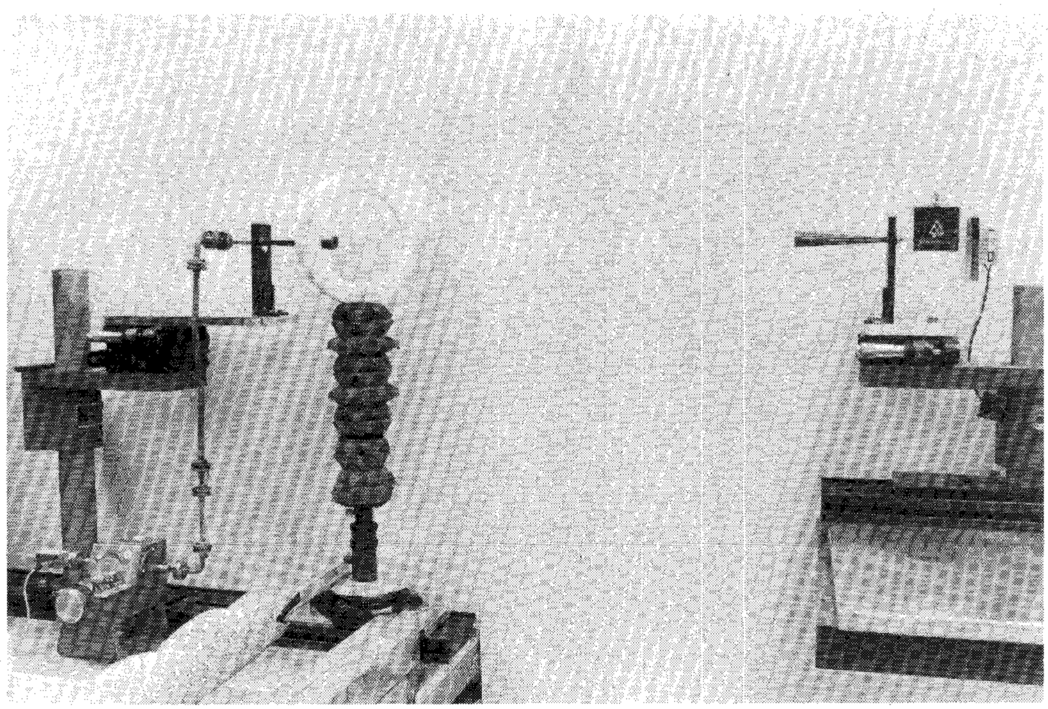

Fig. 4. Photograph of experimental setup. The dielectric sample is mounted in the teflon holder.

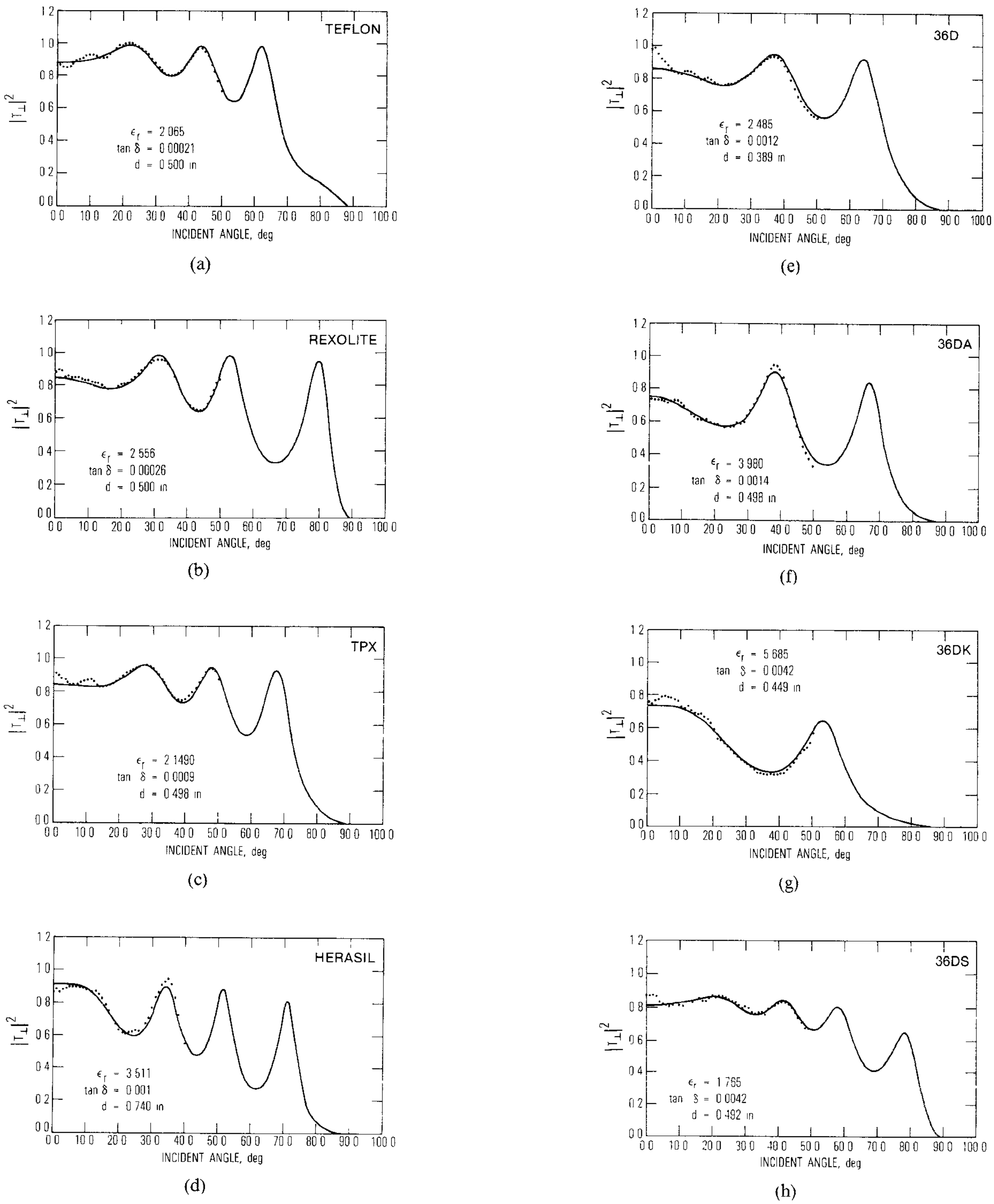

Fig. 5.(a)–(h) The measured power transmission for different dielectric samples are shown by dots. The line curves are the calculated $|T_\perp|^2$ using the best-fit estimates of ϵ_r and $\tan\delta$.

surements of other reported low-loss dielectric materials are shown. These include herasil, a man-made fused quartz, and several casting resins manufactured by Emerson and Cuming, Inc. The theoretical power transmission curves $|T|^2$ obtained from (1) are shown along with the measured points. The plotted curves are obtained from the best-fit bootstrap estimates, which will be discussed in the next section. All measurements are normalized to the signal level without the dielectric; however, the insertion of a dielectric slab into the measurement path increases the power density at the receiving horn. The change in power density depends on the geometry and on the dielectric, and amounted to a few percent correction for the experiments described in this paper. The expression for the correction factor is given in the Appendix. In Fig. 5(a)–(h), these corrections have been applied to the measured points. The zero angle position was determined by auto-collimating a laser beam, co-aligned with the horns, off the slab surface.

To insure that angular biases were removed, the transmission measurements were made with the samples rotated clockwise and counter-clockwise and the two readings at each corresponding angle were averaged.

IV. Discussion of Results

The measurement results were analyzed in the following way. The statistical model was assumed to be of the form

$$y_i = g_i(v) + w_i, \qquad i = 1, 2, \cdots, N \tag{7}$$

where y_i is the ith power transmission measurement at incident angle θ_i and $\theta_i = i - 1$, in degrees. The nonlinear function $g_i(v)$ is the expression $|T|^2$, derived from (1), and v is a vector of two parameters, ϵ_r (relative permittivity) and $\tan\delta$ (loss tangent). The wavelength λ, the slab thickness d, and the angle of incidence θ_i are assumed to be known for each observation. The w_i's are the errors and are assumed to be independent and identically distributed from some distribution. There are systematic errors (e.g., near zero incident angle), and the assumption that these errors are random given overestimates of the standard errors.

The relative permittivity and the loss tangent are estimated by computing $g_i(v)$ at each i for various trial values of ϵ_r and $\tan\delta$. The values of ϵ_r and $\tan\delta$ which minimize

$$S^2 = \frac{1}{51} \sum_{i=1}^{51} (y_i - g_i(v))^2 \tag{8}$$

are taken to be the least-squares estimates (for herasil, 41 replaces 51). The residuals are computed for each observation as

$$r_i = y_i - g_i(\hat{v}) \tag{9}$$

where $\hat{v}$ is the least-squares estimate of v. The bootstrap technique (Efron [23], Efron and Gong [24]) is then used to estimate the standard error of the least-squares estimate of ϵ_r and $\tan\delta$. This is done by the following procedure. A bootstrap sample is generated by

$$y_{bi} = g_i(\hat{v}) + r_{bi}, \qquad i = 1, 2, 3, \cdots, 51 \tag{10}$$

where $r_{bi} = r_j$ with probability 1/51 for $j = 1, 2, \cdots, 51$. A bootstrap estimate $\hat{v}_n$ is obtained for each n by applying the least-squares approach to the bootstrap sample. This procedure is replicated B times. B was chosen to be 20 for this application. The bootstrap estimate of v is then

$$\hat{v}_b = \frac{1}{20} \sum_{n=1}^{20} \hat{v}_n \tag{11}$$

and the bootstrap estimate of the covariance matrix is

$$\mathrm{cov}_b = \frac{1}{19} \sum_{n=1}^{20} (\hat{v}_n - \hat{v}_b)(\hat{v}_n - \hat{v}_b)^T \tag{12}$$

where T is the transpose. The estimates of the standard error of the least-squares estimates of ϵ_r and $\tan\delta$ are obtained directly from cov_b.

Table I gives a summary of the analysis for the dielectrics measured. The materials 36D, 36DA, 36DK, and 36DS are low-loss casting resins manufactured by Emerson–Cuming, Inc. The number in parentheses for these resins are the permittivities and loss tangents reported by the manufacturer for lower frequencies.

TABLE I
ESTIMATES OF PERMITTIVITIES AND LOSS TANGENTS
$F = 93.788$ GHz

Material	Least Squares Estimate		Bootstrap Estimates With Standard Error	
	ϵ_r	tan δ	ϵ_r	tan δ
Teflon	2.065	.0002	2.065 ± .004	.00021 ± .00003
Rexolite	2.556	.0003	2.556 ± .005	.00026 ± .00006
TPX	2.150	.0010	2.149 ± .005	.0009 ± .0001
Herasil (fused quartz)	3.510	.0010	3.511 ± .005	.0010 ± .0001
36D	2.485 (2.45)	.0012 (<.0007)	2.487 ± .008	.0011 ± .0002
36DA	3.980 (3.7)	.0012 (<.0007)	3.980 ± .009	.0014 ± .0001
36DK	5.685 (5.4)	.0040 (<.0008)	5.685 ± .009	.0042 ± .0001
36DS	1.765 (1.9)	.0042 (<.001)	1.766 ± .006	.0041 ± .0001

TABLE II
COMPARISONS WITH OTHER PERMITTIVITY MEASUREMENTS

Reference	Frequency (GHz)	Teflon ϵ_r	Teflon tan δ	Rexolite ϵ_r	Rexolite tan δ	TPX ϵ_r	TPX tan δ
This paper	93.8	2.065	.00021	2.556	.00026	2.149	.0009
[6]	94.8	2.04	.009	2.6	.0026		
[9]	143	2.07		2.44			
[10]	35*	1.952	.000048				
[12]	35**	1.956	.000047				
[13]	34.5	1.95	.000047			2.126	.00048
[20]	~120	2.054	.0008				
[20]	~300					2.1316	.0016
[21]	~1000					2.1211	.0127

*open resonator method
**cavity method

The determination of the real part of the complex permittivity is sensitive to the wavelength and thickness of the dielectric sample, but is relatively insensitive to errors in the angle of incidence. As mentioned before, the wavelength can be measured very accurately and, in the analysis, it is assumed that this quantity is known exactly. The average of five measured thicknesses was used as the nominal thickness of the dielectric sample, assuming a uniformly distributed error in the range ± 0.001 in about the nominal value. The uncertainty in the thickness is the largest source of error in estimating the relative permittivity, but in practice, this source of error can be further reduced by fabricating a Fabry–Perot plate to tolerances less than that obtained in this study. Also, using the best estimate of the nominal thickness reduces the standard errors in Table I for ϵ_r approximately by a factor of 2. An assumption of a random error of 0.25° rms in the angle measurement has essentially no effect on the results.

In Table II, the values of ϵ_r and $\tan\delta$ determined in this study are compared with other measurements of the common materials. In the table are listed the reference, the measured permittivities, and the frequencies at which the measurements were made.

The results in Table I show that, for the best measurements, the standard errors in the determination of ϵ_r and $\tan\delta$ are 0.2 and 2.5 percent, respectively. The method described in this paper for measuring the complex permittivity of materials is relatively simple, yet, if care is exercised, still gives degrees of precision comparable to the best obtained by other techniques.

V. Conclusions

Using a quasi-optical method, the complex permittivity of materials can be determined by measuring the power transmission of a perpendicularly polarized wave through a Fabry–Perot etalon fabricated out of the sample dielectric, at different angles of incidence. Accurate determinations are obtained by measuring the signal frequency accurately, and by machining the etalon to close tolerances. Errors due to extraneous reflections into the measurement path are reduced by using large dielectric samples and use of absorbing material at suitable locations. Estimates of the standard errors in the determinations of the relative permittivity and loss tangent are obtained by using a bootstrap resampling technique.

Appendix

In the actual experiment, the incident signal was not a plane wave but a spherical wave. The transmitter and receiver were sufficiently far apart that the calculated results as given by (1) were not affected by the spherical wave. However, the insertion of a dielectric in the ray path increases the power density at the receiver, and the increase in power density has to be taken into account. The change in power density can be calculated in the following way. As viewed geometrically from the transmitter, the receiver horn subtends an angle 2α. With the dielectric slab inserted in the ray path, using ray tracing, rays diverging from the transmitter at an angle slightly greater than 2α now intersect the edges of the receiver horn. If this new angle is called γ, the ratio of the power densities, with and without the dielectric slab is given by the square of the ratio of the subtended angles, $(2\alpha/\gamma)^2$. If P_0 is the power density without the slab, and P_s is that with the slab

$$\frac{P_0}{P_s} = \left\{1 + \frac{d}{a}\left[\frac{\sin(|\theta-\alpha| - \beta_1)}{\cos\alpha\cos\beta_1} - \frac{\sin(\theta+\alpha-\beta_2)}{\cos\alpha\cos\beta_2}\right]\right\}^{-2}$$

where

$$\beta_1 = \sin^{-1}\left[\frac{\sin(\theta-\alpha)}{n}\right]$$

$$\beta_2 = \sin^{-1}\left[\frac{\sin(\theta+\alpha)}{n}\right]$$

$n = \sqrt{\epsilon_r}$, the index of refraction of the dielectric sample

and

θ angle of incidence for the axial ray,
2α geometric angle subtended by receiver horn as viewed from transmitter horn,
a receiver horn dimension,
d thickness of dielectric slab.

Acknowledgment

The authors wish to thank G. G. Berry for his help in fabricating components and fixtures for this project, and the referee who made some helpful suggestions.

References

[1] R. M. Redheffer, "The measurements of dielectric constants," in *Technique of Microwave Measurements*, C. G. Montgomery, Ed. New York: McGraw-Hill, 1947, ch. 10.
[2] N. W. B. Stone, J. E. Harries, D. W. E. Fuller, J. G. Edwards, A. E. Costley, J. Chamberlain, T. G. Blaney, J. R. Birch, and A. E. Bailey, "Electrical standards of measurement: Part 3: Submillimetre-wave measurements and standards," *Proc. IEEE*, vol. 122, no. 10R, pp. 1054–1070, 1975.
[3] M. J. Bangham, J. R. Birch, T. G. Blaney, A. E. Costley, J. E. Harries, R. G. Jones, and N. W. B. Stone, "Physical measurements in the 100–1000 GHz range," *Radio Electron. Eng.*, vol. 49, pp. 403–417, 1979.
[4] M. N. Afsar, J. Chamberlain, and G. W. Chantry, "High-precision dielectric measurement on liquids and solids at millimeter and submillimeter wavelengths," *IEEE Trans. Instrum. Meas.*, vol. IM-25, pp. 290–294, 1976.
[5] M. N. Afsar and K. J. Button, "Precise millimeter-wave measurements of complex refractive index, complex dielectric permittivity and loss tangent of GaAs, Si, SiO_2, Al_2O_3, BeO, Macor, and Glass," *IEEE Trans. Microwave Theory Tech*, vol. MTT-31, pp. 217–223, Feb. 1983.
[6] W. B. Bridges, M. B. Klein, and E. Schweig, "Measurement of the dielectric constant and loss tangent of thallium mixed halide crystals KRS-5 and KRS-6 at 95 GHz," *IEEE Trans. Microwave Theory Tech.*, vol. MTT-30, pp. 286–292, Mar. 1982.
[7] S. Roberts and A. von Hippel, "A new method for measuring dielectric constant and loss in the range of centimeter waves," *J. Appl. Phys.*, vol. 17, pp. 610–616, July 1946.
[8] W. Culshaw and M. V. Anderson, "Measurement of dielectric constants and losses with a millimeter wave Fabry-Perot interferometer," NBS Rep. 8786, 1961.
[9] J. E. Degenford and P. D. Coleman, "A quasi-optics perturbation technique for measuring dielectric constants," *Proc. IEEE*, vol. 54, pp. 520–522, 1966.
[10] C. A. Balanis, "Dielectric constant and loss tangent measurements at 60 and 90 GHz using the Fabry–Perot interferometer," *Microwave J.*, vol. 14, pp. 39–44, 1971.
[11] A. L. Cullen and P. K. Yu, "The accurate measurement of permittivity by means of an open resonator," *Proc. Roy. Soc. London* A., vol. 325, pp. 493–509, 1971.
[12] R. J. Cook, R. G. Jones, and C. B. Rosenberg, "Comparison of cavity and open-resonator measurements of permittivity and loss angle at 35 GHz," *IEEE Trans. Instrum. Meas.*, vol. IM-23, pp. 438–442, 1974.
[13] R. G. Jones, "Precise dielectric measurements at 35 GHz using an open microwave resonator," *Proc. Inst. Elec. Eng.*, vol. 123, pp. 285–290, 1976.
[14] T. E. Talpey, "Optical methods for the measurement of complex dielectric and magnetic constants at centimeter and millimeter wavelengths," *IRE Trans. Microwave Theory Tech.*, vol. MTT-2, pp. 1–12, 1954.
[15] J. E. Chamberlain and H. A. Gebbie, "Determination of the refractive index of a solid using a far infra-red maser," *Nature*, vol. 206, pp. 602–603, 1965.
[16] J. E. Chamberlain, J. Haigh, and M. J. Hine, "Phase modulation in far infrared (submillimeter-wave) interferometers. III-laser refractometry," *Infrared Phys.*, vol. 11, pp. 75–84, 1971.

[17] J. E. Chamberlain, J. E. Gibbs, and H. A. Gebbie, "Refractometry in the far infra-red using a two-beam interferometer," *Nature*, vol. 198, pp. 874–875, 1963.
[18] K. H. Breeden and A. P. Sheppard, "Millimeter and submillimeter wave dielectric measurements," *Microwave J.*, vol. 10, no. 12, pp. 59, 1967.
[19] J. Chamberlain, J. E. Gibbs, and H. A. Gebbie, "The determination of refractive index spectra by Fourier spectrometry," *Infrared Phys.*, vol. 9, pp. 185–209, 1969.
[20] E. E. Bell, "Measurement of the far infrared optical properties of solids with a Michelson interferometer used in the asymmetric mode," *Infrared Phys.*, vol. 6, p. 57–74, 1966.
[21] J. R. Birch, J. D. Dromey, and J. Lesurf, "The optical constants of some common low-loss polymers between 4 and 40 cm^{-1}," *Infrared Phys.*, vol. 21, pp. 225–228, 1981.
[22] D. S. Jones, *The Theory of Electromagnetism.* New York: Macmillan, 1964, ch. 6.
[23] B. Efron, *The Jackknife, the Bootstrap, and Other Resampling Plans* (CBMS-NSF Reg. Conf. Series Appl. Math) vol. 38. Philadelphia, PA: Soc. Ind. App. Math, 1982.
[24] B. Efron and G. Gong, "A leisurely look at the bootstrap, the jackknife, and cross-validation," *Amer. Statistician*, vol. 37, pp. 36–48, 1983.

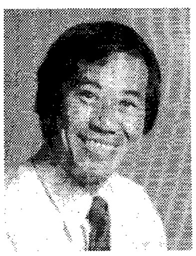

Fred I. Shimabukuro (M'56) was born in Honolulu, HI, on September 3, 1932. He received the B.S. and M.S. degrees in electrical engineering from M.I.T., Cambridge, MA, in 1955 and 1956, respectively, and the Ph.D degree from Caltech, Pasadena, CA, in 1962.

He worked at the Hughes Aircraft Company from 1956 to 1958, and, since 1962, has been employed at The Aerospace Corporation in El Segundo, CA. His current research activity is in millimeter and submillimeter wave technology.

Dr. Shimabukuro is a member of Sigma Xi.

Steven Lazar (M'80) was born in Brooklyn, NY, in 1958. He received the M.S. degree in electrical engineering, concurrently with the B.S. degree in electrical engineering, from the University of California at Los Angeles in 1979.

Since 1979, he has been a Member of the Technical Staff at The Aerospace Corporation in El Segundo, CA. He is currently active in computer-aided microwave circuit design and in millimeter-wave radiometry.

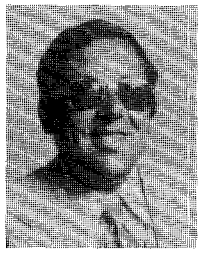

Michael R. Chernick was born in Havre de Grace, MD, on March 11, 1947. He received the B.S. degree from the State University of New York at Stony Brook in 1969, the M.A. degree from the University of Maryland College Park, in 1973, and the M.S. and Ph.D. degrees from Stanford University, Stanford, CA, in 1976 and 1978, respectively.

He is currently a Member of the Technical Staff at The Aerospace Corporation in El Segundo, CA, and is also a Lecturer in the Department of Management Science at California State University at Fullerton. His main interest is in applied statistics, particularly applications to time series and classification problems.

Dr. Chernick is a member of the American Statistical Association, the Institute of Mathematical Statistics, the American Mathematical Society, the Bernoulli Society, and the Society for Industrial and Applied Mathematics.

Howell B. Dyson was born in San Diego, CA, on March 9, 1932. He received the A.A. degree in engineering from Orange Coast College of Costa Mesa, CA, in 1953.

He has worked at the Haliburton Corporation (1956–1960) and at the Raymond De-Icer Engineering Company (1960–1964). Since 1964 he has been employed at The Aerospace Corporation in El Segundo, CA, engaged in research and development of millimeter-wave components and radiometers.